Chapter 8
Light-Sensitive Belousov–Zhabotinsky Computing Through Simulated Evolution

Larry Bull, Rita Toth, Chris Stone, Ben De Lacy Costello and Andrew Adamatzky

Abstract Many forms of unconventional computing, i.e., massively parallel non-linear computers, can be realised through simulated evolution. That is, the behaviour of non-linear media can be controlled automatically and the structural design of the media optimized through the nature-inspired machine learning approach. This chapter describes work using the Belousov–Zhabotinsky reaction as a non-linear chemical medium in which to realise computation. A checkerboard image comprising of varying light intensity cells is projected onto the surface of a catalyst-loaded gel resulting in rich spatio-temporal chemical wave behaviour. Cellular automata are evolved to control the chemical activity through dynamic adjustment of the light intensity, implementing a number of Boolean functions in both simulation and experimentation.

8.1 Introduction

Excitable and oscillating chemical system—the Belousov–Zhabotinsky (BZ) reaction [35]—have been used to solve a number of computational tasks such as implementing logical circuits [3, 31], image processing [22], shortest path problems [30] and memory [27]. In addition chemical diodes [4], coincidence detectors [15] and transformers where a periodic input signal of waves may be modulated by the barrier

L. Bull (✉) · C. Stone · A. Adamatzky
Department of Computer Science, University of the West of England, Bristol, UK
e-mail: larry.bull@uwe.ac.uk

A. Adamatzky
e-mail: andrew.adamatzky@uwe.ac.uk

B. De Lacy Costello
Institute of BioSensing Technology, University of the West of England, Bristol, UK
e-mail: ben.delacycostello@uwe.ac.uk

R. Toth
High Performance Ceramics, EMPA, Dubendorf, Switzerland
e-mail: Rita.Toth@empa.ch

A. Adamatzky (ed.), *Advances in Unconventional Computing*,
Emergence, Complexity and Computation 23,
DOI 10.1007/978-3-319-33921-4_8

into a complex output signal depending on the gap width and frequency of the input [28] have all been demonstrated experimentally.

A number of experimental and theoretical constructs utilising networks of chemical reactions to implement computation have been described. These chemical systems act as simple models for networks of coupled oscillators such as neurons, circadian pacemakers and other biological systems [21]. Ross and co-workers [5] produced a theoretical construct suggesting the use of "chemical" reactor systems coupled by mass flow for implementing logic gates neural networks and finite-state machines. In further work Hjelmfelt et al. [16, 17] simulated a pattern recognition device constructed from large networks of mass-coupled chemical reactors containing a bistable iodate-arsenous acid reaction. They encoded arbitrary patterns of low and high iodide concentrations in the network of 36 coupled reactors. When the network is initialized with a pattern similar to the encoded one then errors in the initial pattern are corrected bringing about the regeneration of the stored pattern. However, if the pattern is not similar then the network evolves to a homogenous state signalling non-recognition.

In related experimental work Laplante et al. [23] used a network of eight bistable mass coupled chemical reactors (via 16 tubes) to implement pattern recognition operations. They demonstrated experimentally that stored patterns of high and low iodine concentrations could be recalled (stable output state) if similar patterns were used as input data to the programmed network. This highlights how a programmable parallel processor could be constructed from coupled chemical reactors. This described chemical system has many properties similar to parallel neural networks. In other work Lebender and Schneider [24] described methods of constructing logical gates using a series of flow rate coupled continuous flow stirred tank reactors (CSTR) containing a bistable nonlinear chemical reaction. The minimal bromate reaction involves the oxidation of cerium(III) (Ce^{3+}) ions by bromate in the presence of bromide and sulphuric acid. In the reaction the Ce^{4+} concentration state is considered as "0" ("False") and "1" ("True") if a given steady state is within 10 % of the minimal (maximal) value. The reactors were flow rate coupled according to rules given by a feedforward neural network run using a PC. The experiment is started by feeding in two "true" states to the input reactors and then switching the flow rates to generate "true"-"false", "false"-"true" and "false"-"false". In this three coupled reactor system the AND (output "true" if inputs are both high Ce^{4+}, "true"), OR (output "true" if one of the inputs is "true"), NAND (output "true" if one of the inputs is "false") and NOR gates (output "true" if both of the inputs are "false") could be realised. However to construct XOR and XNOR gates two additional reactors (a hidden layer) were required. These composite gates are solved by interlinking AND and OR gates and their negations. In their work coupling was implemented by computer but they suggested that true chemical computing of some Boolean functions may be achieved by using the outflows of reactors as the inflows to other reactors, i.e., serial mass coupling.

As yet no large scale experimental network implementations have been undertaken mainly due to the complexity of analysing and controlling many reactors. That said there have been many experimental studies carried out involving coupled oscillating

and bistable systems (e.g., see [6, 10, 18, 32]). The reactions are coupled together either physically by diffusion or an electrical connection or chemically, by having two oscillators that share a common chemical species. The effects observed include multistability, synchronisation, in-phase and out of phase entrainment, amplitude or "oscillator death", the cessation of oscillation in two coupled oscillating systems, or the converse, "rhythmogenesis", in which coupling two systems at steady state causes them to start oscillating [11].

Alongside the development of unconventional computers has been the growing use of machine learning techniques to aid their design and programming (see [25] for an overview). Since techniques such as evolutionary computing (e.g., [12]) have been shown able to handle various complex tasks effectively, the aim is to apply them to harness the as yet only partially understood intricate dynamics of non-linear media to perform computations more effectively than with traditional architectures. Previous theoretical and experimental studies have shown that reaction-diffusion chemical systems are capable of information processing. As such, we have been exploring the use of simulated evolution to design such chemical systems which exploit collision-based computing (e.g., [1]). We use a spatially-distributed light-sensitive form of the BZ reaction in gel which supports travelling reaction-diffusion waves and patterns. Exploiting the photoinhibitory property of the reaction, the chemical activity (amount of excitation on the gel) can be controlled by an applied light intensity, namely it can be decreased by illuminating the gel with high light intensity and vice versa. In this way a BZ network is created via light and controlled using (heterogeneous) cellular automata (CA) designed using simulated evolution [8, 9, 14]. This architecture is adapted from the system described in [34] and experimental chemical computers have been realised, as will be described.

8.2 Simulated Media

We use two-variable Oregonator equation [13] adapted to a light-sensitive Belousov–Zhabotinsky (BZ) reaction with applied illumination [7]:

$$\begin{aligned} \frac{\partial u}{\partial t} &= \frac{1}{\varepsilon}(u - u^2 - (fv + \phi)\frac{u - q}{u + q}) + D_u \nabla^2 u \\ \frac{\partial v}{\partial t} &= u - v \end{aligned} \tag{8.1}$$

The variables u and v represent the instantaneous local concentrations of the bromous acid autocatalyst and the oxidized form of the catalyst, $HBrO_2$ and tris (bipyridyl) Ru (III), respectively, scaled to dimensionless quantities. The rate of the photo-induced bromide production is designated by ϕ, which also denotes the excitability of the system in which low simulated light intensities facilitate excitation while high intensities result in the production of bromide that inhibits the process, experimentally verified by [19]. The system was integrated using the Euler method

with a five-node Laplacian operator, time step $\Delta t = 0.001$ and grid point spacing $\Delta x = 0.62$. The diffusion coefficient, D_u, of species u was unity, while that of species v was set to zero as the catalyst is immobilized in the gel. The kinetic parameters were set to $\varepsilon = 0.11, f = 1.1$ and $q = 0.0002$. The medium is oscillatory in the dark which made it possible to initiate waves in a cell by setting its simulated light intensity to zero. At different ϕ values the medium is excitable, sub-excitable or non-excitable.

8.2.1 Cellular Automata

We have used cellular automata (CA) to control such chemical systems (Fig. 8.1), i.e., finite automata are arranged in a two-dimensional lattice with aperiodic boundary conditions (an edge cell has five neighbours, a corner cell has three neighbours, all other cells have eight neighbours each). Use of a CA with such a two-dimensional topology is a natural choice given the spatio-temporal dynamics of the BZ reaction. Each automaton updates its state depending on its own state and the states of its neighbours. States are updated in parallel and in discrete time. In standard CA all cells have the same state transition function (rule), whereas in this work the CA is heterogeneous, i.e., each cell/automaton has its own state transition function. The transition function of every cell is evolved by a simple evolutionary process. This approach is very similar to that presented in [29]. However, his reliance upon each

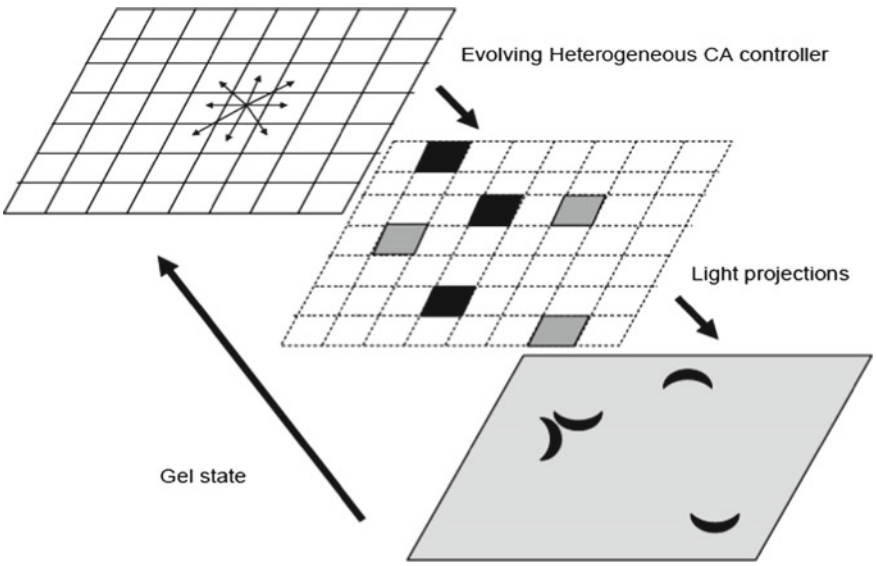

Fig. 8.1 Relationship between the CA controller, applied grid pattern and chemical system comprising one process control cycle. Modified with permission from J. Chem. Phys. 129, 184708 (2008). Copyright 2008, AIP Publishing LLC

cell having access to its own fitness means it is not applicable in the majority of chemical computing scenarios we envisage. Instead, fitness is based on emergent global phenomena in our approach (as in [26], for example). Thus, following [20], we use a simple approach wherein each automaton of the two-dimensional CA controller is developed via a simple genetics-based hillclimber. After fitness has been assigned, some proportion of the CA genes are randomly chosen and mutated. Mutation is the only variation operator used here to modify a given CA cell's transition rule to allow the exploration of alternative light levels for the grid state. For a CA cell with eight neighbours there are 29 possible grid state to light level transitions, each of which is a potential mutation site. After the defined number of such mutations have occurred, an evolutionary generation is complete and the simulation is reset and repeated. The system keeps track of which CA states are visited since mutation. On the next fitness evaluation (at the end of a further 25 control cycles) mutations in states that were not visited are discarded on the grounds that they have not contributed to the global fitness value and are thus untested. We also performed control experiments with a modified version to determine the performance of an equivalent random CA controller. This algorithm ignored the fitness of mutants and retained all mutations except those from unvisited states.

8.2.2 Controller

For a given experiment, a random set of CA rules is created for a two-dimensional array of size 10-by-10 cells. The rule for each cell is represented as a gene in a genome, which at any one time takes one of the discrete light intensity values used in the experiment. As previously mentioned, the grid edges are not connected (i.e., the grid is planar and does not form a toroid) and the neighborhood size of each cell is of radius 1; cells consider neighborhoods of varying size depending upon their spatial position, varying from three in the corners, to five for the other edge cells, and eight everywhere else. In the model each of the 100 cells consists of 400 (20-by-20) simulation points for the reaction. The reaction is thus simulated numerically by a lattice of size 200-by-200 points, which is divided into the 10-by-10 grid.

To begin examining the potential for the evolution of controllers for such temporally dynamic structures in the continuous, non-linear 2D media described we have designed a simple scheme to create a number of two-input Boolean logic gates. Excitation is fed in at the bottom of the grid into a branching pattern. To encode a logical '1' and '0' either both branches or just one branch of the two "trees" shown in Fig. 8.2 are allowed to fill with excitation, i.e., the grid is divided into two for the inputs (Fig. 8.3). These waves were channelled into the grid and broken up into 12 fragments by choosing an appropriate light pattern as shown in Fig. 8.2. The black area represents the excitable medium whilst the white area is non-excitable. After initiation three light levels were used: one is sufficiently high to inhibit the reaction; one is at the sub-excitable threshold such that excitation just manages to propagate; and the other low enough to fully enable it. The modelled chemical system was

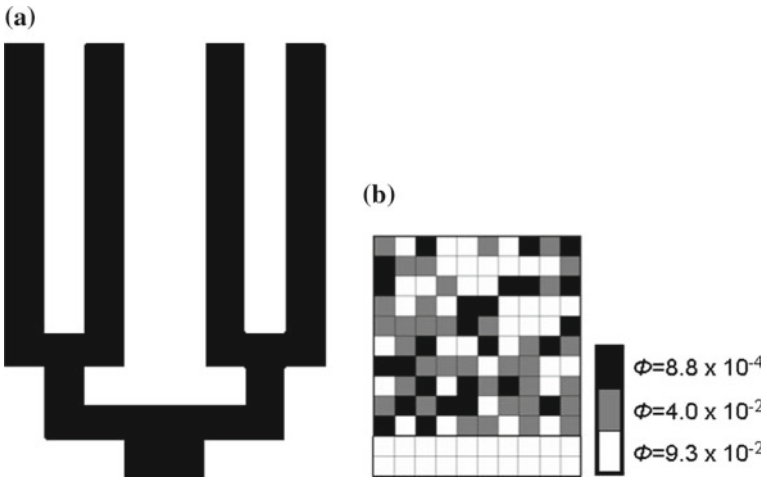

Fig. 8.2 Showing initiation pattern **a** and a typical example of a coevolved light pattern **b**. Modified with permission from J. Chem. Phys. 129, 184708 (2008). Copyright 2008, AIP Publishing LLC

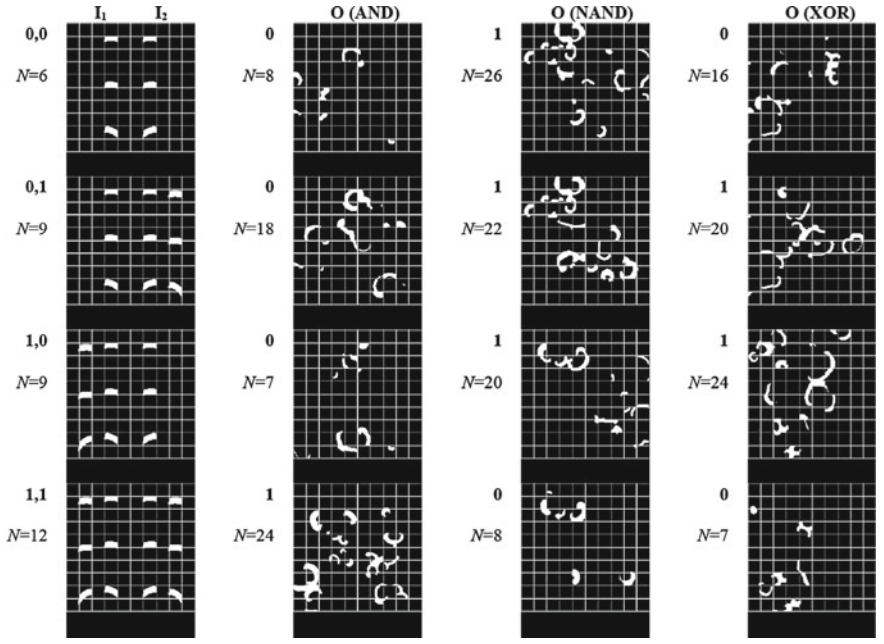

Fig. 8.3 Typical examples of solutions of AND, NAND and XOR logic gates in simulation, required active cells: 20, N: actual number of active cells. Input states I1, I2 for the logic gates are shown on the left and consist of two binary digits, spatially encoded using left and right "initiation trees" (Fig. 8.7). Input values of '0' are encoded using a single branch of the relevant tree resulting in 3 fragments, while binary '1' is encoded using both branches of the tree resulting in 6 fragments. Evolution found a solution in 56 (AND), 364 (NAND) and 16556 (XOR) generations

run for 600 iterations of the simulator. This value was chosen to produce network dynamics similar to those obtained in experiment over 10 s of real time.

8.3 Simulated Experiments

A colour image was produced by mapping the level of oxidized catalyst at each simulation point into an RGB value. Image processing of the colour image was necessary to determine chemical activity. This was done by differencing successive images on a pixel by pixel basis to create a black and white thresholded image. Each pixel in the black and white image was set to white (corresponding to excitation) if the intensity of the red or blue channels in successive colour images differed by more than 5 out of 256 pixels (1.95 %). Pixels at locations not meeting this criterion were set to black. An outline of the grid was superimposed on the black and white images to aid visual analysis of the results.

The black and white images were then processed to produce a 100-bit description of the grid for the CA. In this description each bit corresponds to a cell and it is set to true if the average level of activity within the given cell is greater than a predetermined threshold of 10 %. Here, activity is computed for each cell as the fraction of white pixels in that cell. This binary description represents a high-level depiction of activity in the BZ network and is used as input to the CA. Once cycle of the CA is performed whereby each cell of the CA considers its own state and that of its neighbours (obtained from the binary state description) to determine the light level to be used for that grid cell in the next time step. Each grid cell may be illuminated with one of three possible light levels. The CA returns a 100-digit trinary action string, each digit of which indicates whether high ($\phi = 0.093023$), sub-excitable threshold ($\phi = 0.04$) or low ($\phi = 0.000876$) intensity light should be projected onto the given cell. The progression of the simulated chemical system, image analysis of its state and operation of the CA to determine the set of new light levels comprises one control cycle of the process. A typical light pattern generated by the CA controller is shown in Fig. 8.2b. Another 600 iterations are then simulated with those light-levels projected, etc. until 25 control cycles have passed. The number of active cells in the grid, that is those with activity at or above the 10 % threshold, is used to distinguish between a logical ‘0’ and ‘1’ as the output of the system. For example, in the case of XOR, the controller must learn to keep the number of active cells below the specified level for the 00 and 11 cases but increase the number for the 01 and 10 cases.

Figure 8.3 shows typical examples of each of the three logic gates learned using the simulated chemical system. Each of the four possible input combinations is presented in turn—00 to 11—and for each input combination the system is allowed to develop for 25 control cycles. Fitness for each input pattern is evaluated after the 25 control cycles with each correct output scoring 1, resulting in a maximum possible fitness of 4. Figure 8.4 shows the fitness averaged over ten runs for AND and NAND tasks with mutation rate 4000, and similar results for XOR are shown for mutation rate

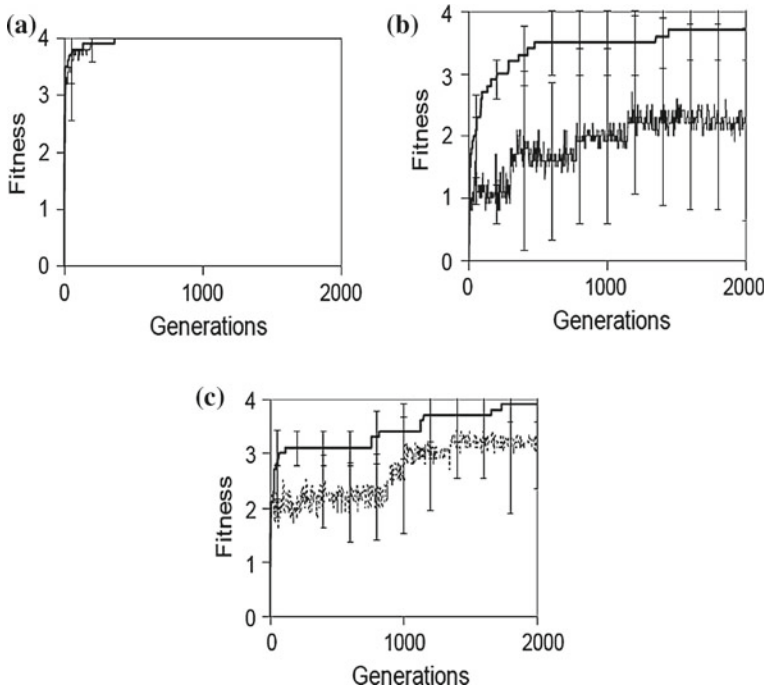

Fig. 8.4 Showing the performance of evolving CA controllers for the three logic gate tasks considered. Dashed lines show the equivalent performance of random search. **a** AND gate. **b** NAND gate. **c** XOR gate

6000. Favourable comparisons to an equivalent random controller are also shown in each case.

8.4 Laboratory Experiments

The success of our simulated experiment encouraged us to build an experimental setup (Fig. 8.5) and perform the same tasks in the real light-sensitive BZ medium. We immobilised the light-sensitive $(Ru(byp)_3{}^{2+}$ catalyst in a thin layer of silica gel which was bathed in the catalyst free BZ reagents. All chemicals were purchased from Aldrich (U.K.) and used as received unless stated otherwise. $Ru(bpy)_3SO_4$ was recrystallised from $Ru(bpy)_3Cl_2$ using sulphuric acid. For the silica gel 222 mL of the purchased 27 % sodium silicate solution (stabilized in 4.9 M sodium hydroxide) was acidified by adding 57 mL of 2 M sulphuric acid and 187 mL of deionised water. Then 0.6 mL of 0.025 M $Ru(bpy)_3SO_4$ and 0.65 mL of 1.0 M sulphuric acid solutions were added to 2.5 mL of the acidified silicate solution. This solution was used to prepare the silica gel in a custom designed 0.3 mm deep Perspex mould. After 3 hours gelation

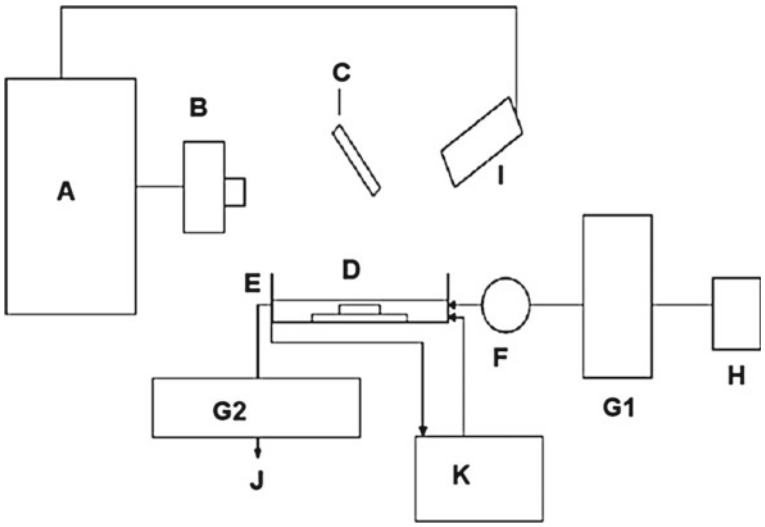

Fig. 8.5 A block diagram of the experimental setup where **a**: computer, **b**: projector, **c**: mirror, **d**: microscope slide with the catalyst-loaded gel, **e**: thermostated Petri dish, **f**: CSTR, **g1** and **g2**: pumps, **h**: stock solutions, **i**: camera, **j**: effluent flow, **k**: thermostated water bath

time the 26 mm × 26 mm × 300 μm gel layers were removed from the mould, carefully washed and stored in water until use. The experiments were performed in a thermostated (22 C^o) open reactor containing the catalyst loaded silica gel and

the catalyst free BZ solution (0.42 M sodium bromate, 0.19 M malonic acid, 0.64 M sulphuric acid and 0.11 M bromide). This reactor was fed by a continuously-fed stirred tank reactor (CSTR) which freshly mixed the BZ reagents to keep the system far from its equilibrium state. The flow between the two reactors and the removal of the effluents was maintained by two peristaltic pumps. An InFocus Model LP820 Projector was used to shine a computer generated 10-by-10 cell checkerboard grid pattern (with a size of 20 mm × 20 mm) on the surface of the gel through a 455 nm narrow bandpass interference filter, 100/100 mm focal length lens pair and mirror assembly (Fig. 8.5). Three light intensity levels were used in the checkerboard image representing excitable, subexcitable threshold, and non-excitable domains, with 0.35, 1.6 and 3.5 mW cm^{-2}, respectively. Images of the chemical wave fragments on the gel were captured using a Lumenera Infinity2 USB 2.0 scientific digital camera. To improve visibility and enable subsequent image processing images were captured while a uniform grey level of 3.5 mW cm^{-2} was projected on the gel for 10 ms instead of the checkerboard grid. Captured images were processed to identify activity in the same way as for the model.

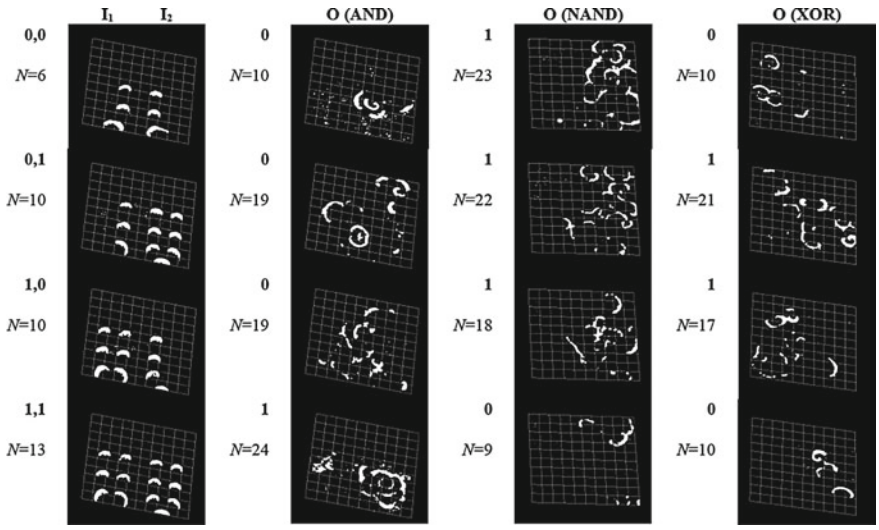

Fig. 8.6 Typical examples of solutions of AND, NAND and XOR logic gates in chemical experiment, required number of active cells: 15 (20 for AND), N: actual number of active cells. Input states I1, I2 for the logic gates are shown on the left and consist of two binary digits, spatially encoded using left and right "initiation trees" (Fig. 8.7a). Input values of '0' are encoded using a single branch of the relevant tree resulting in 3 or 4 fragments, while binary '1' is encoded using both branches of the tree resulting in 6 or 7 fragments. The simulated evolution—seeded with a CA evolved during the simulated runs—found a solution in 16 generations in each case

Figures 8.6 and 8.7 show how similar performance is possible on the real chemical system for each of the three logic functions. In order to produce working XOR and NAND gates from these experiments, it was necessary to use a value of 15 for the

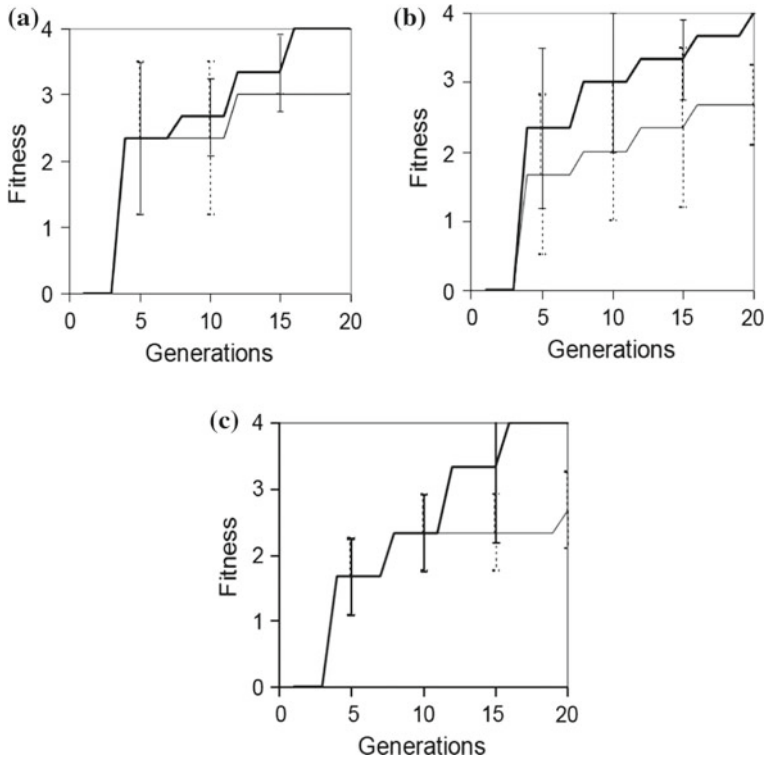

Fig. 8.7 Showing the performance of evolving CA controllers for the three logic gate tasks considered. *Dashed lines* show the equivalent performance of random search. **a** AND gate. **b** NAND gate. **c** XOR gate

required number of active cells due to the relative difficulty of these tasks. All other parameters were the same as those used for numerical simulation.

Because of the limited lifetime of the medium these runs were seeded with CA evolved during the simulated runs presented in Fig. 8.3. Runs using random initial controllers were also explored on the real chemical system (dashed lines on Fig. 8.7), but no successful runs were found over the 40 generations. This is not surprising considering that the average generations needed to find a good solution was higher than 40 in the simulations because of the relative increase in difficulty. Nevertheless the two systems are very similar since the runs with seeded CA evolved during the simulations found solutions in a very short time, namely in 16 or 20 generations. If a solution had been found in four generations it would have meant that the initial states of the simulated and real chemical system are perfectly identical. However, since there is a noticeable difference between the initial states, the solution found by the evolutionary algorithm in simulation was very close to the solution needed for the real chemistry, but a few generations of evolution were needed to adapt to the difference between the two systems. These results show that the approach is capable of adapting to small changes in its environment and finding a solution very quickly when presented with domain-specific knowledge obtained from modeling.

8.5 Conclusion

Excitable and oscillating chemical systems have previously been used to solve a number of simple computational tasks. However, the experimental design of such systems has typically been non-trivial. In this chapter we have presented results from a methodology by which to achieve the complex task of designing such systems—through the use of simulated evolution. We have shown using both simulated and real systems that it is possible in this way to control dynamically the behavior of the BZ reaction, and to design the topology of a network-based approach to chemical computing. As discussed in [25], evolution can also be used to pre-configure programmable/changeable elements of an unconventional medium, such as voltages within liquid crystal, before computation occurs. We have used a similar approach for the gel-based system described above, enabling evolution to predefine where fragment waves of excitation can enter a central area of collision/computation (e.g.,

[33]). Which of these approaches is best able to exploit the properties of non-linear media for computation—or whether their use in combination is possible—remains open to future exploration.

References

1. Adamatzky, A. (ed.): Collision-based Computing. Springer, London (2002)
2. Adamatzky, A., De Lacy Costello, B., Asai, T.: Reaction-Diffusion Computers. Elsevier, Amsterdam (2005)
3. Adamatzky, A., Holley, J., Bull, L., De Lacy Costello, B.: On computing in fine-grained compartmentalised Belousov–Zhabotinsky medium. Chaos, Solitons Fractals **44**(10), 779–790 (2011)
4. Agladze, K., Aliev, R.R., Yamaguhi, T., Yoshikawa, K.: Chemical diode. J. Phys. Chem. **100**, 13895–13897 (1996)
5. Arkin, A., Ross, J.: Computational functions in biochemical reaction networks. Biophys. J. **67**(2), 560–578 (1994)
6. Bar-Eli, K., Reuveni, S.: Stable stationary-states of coupled chemical oscillators: Experimental evidence. J. Phys. Chem. **89**, 1329–1330 (1985)
7. Beato, V., Engel, H.: Pulse propagation in a model for the photosensitive Belousov-Zhabotinsky reaction with external noise. In: Proceedings of the SPIE's First International Symposium on Fluctuations and Noise. International Society for Optics and Photonics (pp. 353-362). (May, 2003)
8. Bull, L.: Evolving Boolean networks on tuneable fitness landscapes. IEEE Trans. Evol. Comput. **16**(6), 817–828 (2012)
9. Bull, L.: Using genetical and cultural search to design unorganised machines. Evol. Intell. **5**(1), 23–33 (2012)
10. Crowley, M.F., Field, R.J.: Electrically coupled Belousov–Zhabotinsky oscillators 1: experiments and simulations. J. Phys. Chem. **90**, 1907–1915 (1986)
11. Dolnik, M., Epstein, I.R.: Coupled chaotic oscillators. Phys. Rev. E **54**, 3361–3368 (1996)
12. Eiben, A., Smith, J.: Introduction to Evolutionary Computing. Springer, Heidelberg (2003)
13. Field, R.J., Noyes, R.M.: Oscillations in chemical systems. IV. Limit cycle behavior in a model of a real chemical reaction. J. Chem. Phys. **60**(5), 1877–1884 (1974)
14. Fogel, L. J., Owens, A.J., Walsh, M.J. Artificial intelligence through a simulation of evolution. In M. Maxfield et al. (Eds.) Biophysics and Cybernetic Systems: Proceedings of the 2nd Cybernetic Sciences Symposium. pp. 131–155. Spartan Books (1965)
15. Gorecki, J., Yoshikawa, K., Igarashi, Y.: On chemical reactors that can count. J. Phys. Chem. A **107**, 1664–1669 (2003)
16. Hjelmfelt, A., Weinberger, E.D., Ross, J.: Chemical implementation of neural networks and turing machines. PNAS **88**, 10983–10987 (1991)
17. Hjelmfelt, A., Ross, J.: Mass-coupled chemical systems with computational properties. J. Phys. Chem. **97**, 7988–7992 (1993)
18. Holz, R., Schneider, F.W.: Control of dynamic states with time-delay between 2 mutually flow-rate coupled reactors. J. Phys. Chem. **97**, 12239 (1993)
19. Kadar, S., Amemiya, T., Showalter, K.: Reaction mechanism for light sensitivity of the $Ru(bpy)_3^{2+}$ -catalyzed Belousov-Zhabotinsky reaction. J. Phys. Chem. A **101**(44), 8200–8206 (1997)
20. Kauffman, S.A.: The Origins of Order. Oxford Press, Oxford (1993)
21. Kawato, M., Suzuki, R.: Two coupled neural oscillators as a model of the circadian pacemaker. J. Theor. Biol. **86**, 547–575 (1980)
22. Kuhnert, L., Agladze, K.I., Krinsky, V.I.: Image processing using light sensitive chemical waves. Nature **337**, 244–247 (1989)

23. Laplante, J.P., Pemberton, M., Hjelmfelt, A., Ross, J.: Experiments on pattern recognition by chemical kinetics. J. Phys. Chem. **99**, 10063–10065 (1995)
24. Lebender, D., Schneider, F.W.: Logical gates using a nonlinear chemical reaction. J. Phys. Chem. **98**, 7533–7537 (1994)
25. Miller, J., Harding, S., Tufte, G.: Evolution in-matrio: evolving computation in materials. Evol. Intell. **7**(1), 49–67 (2014)
26. Mitchell, M., Hraber, P., Crutchfield, J.: Revisiting the edge of chaos: evolving cellular automata to perform computations. Complex Syst. **7**, 83–130 (1993)
27. Motoike, I.N., Yoshikawa, K., Iguchi, Y., Nakata, S.: Real time memory on an excitable field. Phys. Rev. E **63**, 1–4 (2001)
28. Sielewiesiuk, J., Gorecki, J.: Passive barrier as a transformer of chemical frequency. J. Phys. Chem. A **106**, 4068–4076 (2002)
29. Sipper, M.: Evolution of Parallel Cellular Machines. Springer, Heidelberg (1997)
30. Steinbock, O., Toth, A., Showalter, K.: Navigating complex labyrinths: optimal paths from chemical waves. Science **267**, 868–871 (1995)
31. Steinbock, O., Kettunen, P., Showalter, K.: Chemical wave logic gates. J. Phys. Chem. **100**, 18970–18975 (1996)
32. Stuchl, I., Marek, M.: Dissipative structures in coupled cells: experiments. J. Phys. Chem. **77**, 2956–2963 (1982)
33. Toth, R., Stone, C., De Lacy Costello, B., Adamatzky, A., Bull, L.: Simple collision-based chemical logic gates with adaptive computing. J. Nanotechnol. Mol. Comput. **1**(3): 1–16 (2009)
34. Wang, J., Kádár, S., Jung, P., Showalter, K.: Noise driven avalanche behavior in subexcitable media. Phys. Rev. Lett. **82**, 855–858 (1999)
35. Zaikin, A.N., Zhabotinsky, A.M.: Concentration wave propagation in two-dimensional liquid-phase self-oscillating system. Nature **225**, 535–537 (1970)